International Journal of Power Electronics and Drive Systems (IJPEDS)
Vol. 15, No. 3, September 2024, pp. 1826~1837
ISSN: 2088-8694, DOI: 10.11591/ijpeds.v15.i3.pp1826-1837 ❐ 1826

Passivity-based fuzzy logic approach for optimal power extraction from PMSG-wind energy conversion

Pallavi Chaturvedi, Dheeraj Kumar Palwalia
Department of Electrical Engineering, Rajasthan Technical University, Kota, India

Article Info

Article history:

Received Sep 5, 2023
Revised Mar 4, 2024
Accepted Mar 21, 2024

Keywords:

Dynamical non-linear control
Fuzzy logic controller
Lyapunov stability
MPPT
Passivity
PMSG

ABSTRACT

The preference for permanent magnet synchronous generators (PMSGs) in wind energy conversion systems (WECS) is due to their reliability, compactness, and efficiency. However, designing controllers for PMSG-WECS faces challenges from parameter uncertainties, nonlinearity, and grid integration. To address this, a novel passivity-based nonlinear controller (PBNC) is proposed to precisely track speed and torque. This unique PBNC employs a damped approach to address nonlinearity and integrates a fuzzy logic controller (FLPBNC) for robustness. The chosen strategy shapes energy dynamics using Lyapunov functions. The addition of damping elements ensures Lyapunov stability condition and boosts convergence while keeping the energy functions positive. The system design involves linking passive mechanical and electrical parts in a feedback loop. Meanwhile, for grid integration, a proportional-integral (PI) controller manages DC-link voltage and active power supply to the grid. MATLAB/Simulink simulations confirm the effectiveness of the proposed approach compared to conventional methods.

Corresponding Author:

Pallavi Chaturvedi
Department of Electrical Engineering, Rajasthan Technical University
Kota-324010, Rajasthan, India
Email: pallavichat9@gmail.com

1. INTRODUCTION

Wind energy stands as a prominent pillar among renewable energy sources, harnessing the inexhaustible power of wind to generate electricity [1]. The permanent magnet synchronous generator (PMSG) has gained attention as an efficient direct-driven generator in wind turbines. Its gearless design simplifies mechanical components and maintenance needs while providing precise control for optimized energy extraction from variable wind conditions. However, controlling PMSGs poses a challenge due to their inherent nonlinearities and susceptibility to external factors like varying wind speeds. This complexity demands sophisticated control strategies to optimize energy capture and system stability [2].

In addressing the nonlinearities within PMSG systems, a diverse range of strategies have been explored. Backstepping control seeks to minimize instability and complexity by guiding system dynamics [3]. Fuzzy-logic control utilizes fuzzy rules for parameter adjustment through feedback mechanisms, albeit with some sensitivity to errors [4]. Adaptive control fine-tunes parameters via feedback, although it maintains a degree of susceptibility to errors [5]. Sliding mode control is adept at managing disturbances, although it may introduce chattering effects [6]. Intelligent control capitalizes on neural networks to facilitate learning, often demanding substantial computational resources [7]. Fuzzy sliding mode control harmonizes fuzzy logic and sliding mode control to effectively handle uncertainties [8]. Active disturbance rejection control (ADRC) treats parameter uncertainties as disturbances, bolstering overall robustness [9]. Second-order sliding mode control focuses on alleviating chattering effects, refining control precision [10]. Lastly, the integration of methods such as nonlinear observer-based second-order sliding mode control with predictive control offers a comprehensive solution to uncertainties, disturbances, and nonlinearities [11]. Each of these strategies presents unique advantages and limitations, encompassing complexity, accuracy, and computational demands.

Passivity-based nonlinear control (PBNC) emerges as a viable approach, emphasizing system stability and energy preservation. PBNC ensures that the system remains passive, leading to inherent stability and well-behaved responses. While it requires thorough system modelling, it addresses nonlinearities effectively [12].

To ensure stability and controlled management of nonlinear terms, various nonlinear control strategies have been rigorously explored. Among them, passivity-based linear feedback control [13] and adaptive passivity-based nonlinear control stand out. Passivity based sliding control and innovative combinations like passivity-based control (PBC) merged with fuzzy logic control and sliding-mode control [14] also play a pivotal role. These approaches collectively lead to an enhanced PMSG-based systems, thereby boosting performance, stability, and efficiency. However, challenges persist due to intricate controller designs, sensitivity to parameter fluctuations, and the need to address uncertainties and disturbances. In spite of these hurdles, passivity-based control (PBC) introduces an energy-centric approach, reshaping natural energy within the system and introducing necessary damping to achieve control objectives [15]. Beyond PMSG systems, PBC extends its influence to diverse domains including smart grids, buildings, cyber-physical systems, and electric vehicles. Its adaptability and associated advantages make PBC a promising choice for improving system performance across various engineering fields.

In this study, a comprehensive control approach is proposed for permanent magnet synchronous generator (PMSG) systems, addressing various challenges related to the PMSG's non-linear dynamics, time-varying parameters, and external disturbances. The control scheme consists of two main parts: a fuzzy-passivity based control (PBC) system and a classical proportional-integral (PI) control system. The fuzzy-PBC system focuses on optimizing the PMSG's operational speed, rectifying non-linearities, and handling external disturbances and parameter fluctuations. The PI control system regulates the grid-side power and voltage, ensuring reliable and efficient electricity transfer. The proposed approach considers the complete dynamic of the PMSG, emphasizing robustness against parameter variations. This work extends previous research on control strategies for PMSG systems and utilizes the energy-based passivity concept, injecting damping to ensure stability and convergence of measured signals. The proposed approach offers advantages such as a simple control structure, fast convergence, mathematical simplicity, stability, and robustness against parameter variations.

2. METHOD

The configuration in Figure 1 integrates a wind turbine and a PMSG connected to the grid via PWM converters controlled by FLBC and PI controller. Emphasizing the regulation of DC voltage and reactive power, the dynamic equation of the wind turbine-based PMSG is nonlinear, as outlined in next section. Optimal energy extraction is crucial for operational efficiency, and the MSC controller minimizes losses in power transmission, sustaining the DC-link voltage. Simultaneously, grid-side control ensures the exclusive delivery of active power to the grid.

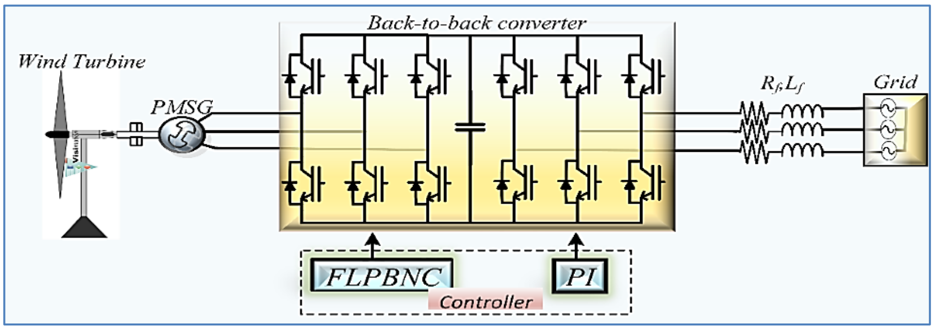

Figure 1. Grid connected PMSG based wind energy conversion system

2.1. Dynamic modelling of PMSG

The representation of permanent magnet synchronous generator in a d-q frame is derived as (1)-(3) [16].

$$v_{dqm} = L_{dqm}\frac{di_{dqm}}{dt} + R_{dqm}i_{dqm} + p\omega_{rtl}(\phi_f + i_{dqm}L_{dq})\xi \quad (1)$$

$$J_m \frac{d\omega_{rtl}}{dt} = T_{mech} - T_{elm} - \text{Ҳ}_{vi}\omega_{rtl} \quad (2)$$

$$T_{elm} = -\frac{3}{2} p \phi_f{}^T \xi \mathrm{i}_{dqm}{}^* \quad (3)$$

These equations feature matrices describing stator voltage (v_{dqm}) and current (i_{dqm}), along with flux (ϕ_f), inductance (L_{dqm}), and resistance (R_S) in the d-q frame as:

$$\begin{bmatrix} \mathrm{v}_{dm} \\ \mathrm{v}_{qm} \end{bmatrix}; \begin{bmatrix} \mathrm{i}_{dm} \\ \mathrm{i}_{qm} \end{bmatrix}; \begin{bmatrix} \emptyset_f \\ 0 \end{bmatrix}; \begin{bmatrix} L_{dm} & 0 \\ 0 & L_{qm} \end{bmatrix}; \begin{bmatrix} R_S & 0 \\ 0 & R_S \end{bmatrix}. \text{Additionally}, \xi = \begin{bmatrix} 0 & -1 \\ 1 & 0 \end{bmatrix}$$

The parameter includes turbine rotor speed ($\omega_{rtl)}$, electromagnetic torque developed (T_{elm}) and moment of inertia turbine (J_m) (viscous friction factor (Ҳ_{vi})) respectively.

2.1.1. PMSG d-q model with linear feedback

The equation defining the relation between flux ϕ_{dq} and current i_{dqm} is given as [17]. Substituting value of i_{dqm} from (4) in (1) gives (5).

$$\phi_{dq} = \begin{bmatrix} \phi_d \\ \phi_q \end{bmatrix} = \left(L_{dq}\mathrm{i}_{dqm} + \phi_f\right) \quad (4)$$

$$\mathrm{v}_{dqm} = \frac{d\phi_{dq}}{dt} + R_{dq}\mathrm{i}_{dqm} + p\omega_{rtl}\left(\phi_{dq}\right)\xi \quad (5)$$

The use of a nonlinear feedback mechanism ensures perpendicular alignment of armature flux with the rotor flux. This approach inherently integrates linearizing feedback by enforcing that the d-axis current (i_{dm}) remains at zero. As a result, the PMSG closely mimics the characteristics of a DC generator. This linearizing feedback can be mathematically described by (6)-(8).

$$\mathrm{v}_{dm} = -p\omega_{rtl}\mathrm{i}_{qm}{}^* \quad (6)$$

Considering $\mathrm{i}_{dm}{}^* = 0$, according to (5) gets reduced to (7).

$$\mathrm{v}_{qm} = \frac{d\phi_q}{dt} + R_q\mathrm{i}_{qm} + p\omega_{rtl}\left(\phi_q\right)\xi \quad (7)$$

While the following PI controller converges the error between i_{qm} and $\mathrm{i}_{qm}{}^*$.

$$\mathrm{v}_{qm} = K_{m_p}\left(\mathrm{i}_{qm}{}^* - \mathrm{i}_{qm}\right) - K_{m_i}\int_0^t\left(\mathrm{i}_{qm}{}^* - \mathrm{i}_{qm}\right) \quad (8)$$

2.1.2. PMSG system dynamics: feedback interconnected electrical and mechanical subsystem

Concept of passivity-based control: The prerequisite to implement passivity requires computation of Euler Lagrange model of PMSG with subsequent selection of suitable input output vector ensuring passive relationship. Thereafter, the system is divided into subsection interlinked through negative feedback [18]. The detailed machine side controller design is illustrated in Figure 2.

The control design comprises of two stages of control. The initial stage of control involves application of fuzzy logic to derive electromagnetic torque. In subsequent stages control voltage is derived after desired current is obtained using electromagnetic torque. For given subsystem, passivity is mathematically represented by an integral inequality [19] as given by (9).

$$\mathcal{E}_m(x) - \mathcal{E}_m(x_0) \leq \int_0^t \mathcal{Y}^T(\tau)\mathcal{u}(\tau d(\tau) \quad (9)$$

This inequality ensures that the input power ($\mathcal{u}^T\mathcal{Y}$) is always greater than or equal to the decrease in storage function, leading to energy dissipation or bounded energy storage. Total stored energy is derived as (10) and (11).

$$\mathcal{E}_{me}\left(\mathrm{i}_{dqm}, \omega_{rtl}\right) = \overbrace{\frac{1}{2}\,\mathrm{i}_{dqm}^T L_{dq}\mathrm{i}_{dqm} + \phi_{dq}{}^{\mathrm{T}}\mathrm{i}_{dqm}}^{electrical\ energy} + \overbrace{\frac{1}{2}J_m\omega_{rtl}{}^2}^{mechanical\ energy} \quad (10)$$

$$\frac{d}{dt}\mathcal{E}_{me}\left(\mathrm{i}_{dqm},\omega_{rtl}\right) = -\frac{d}{dt}\left(\mathrm{i}^T_{dqm}R_m\right) + \frac{d}{dt}\left(\,\phi_{dq}{}^{\mathrm{T}}\mathrm{i}_{dqm}\right) + Y_{em}{}^{T}V_{em} \tag{11}$$

Where, R_m = diag (R_{dq}, X_{vi}) is a symmetrical as well as definite positive matrix. Integrating each side of the above equation along [0, T_{mech}], gives (12).

$$\mathcal{E}_{me}(T_{mech}) - \mathcal{E}_{me}\,(0) = \overbrace{\int_0^{T_{mech}} \mathrm{i}^T_{dqm}R_m\mathrm{i}_{dqm}d\tau}^{dissipated\ energy}$$

$$+\overbrace{\int_0^{T_{mech}} Y_{em}{}^{T}V_{em}d\tau \;+\; \left[\,\phi_{dq}{}^{\mathrm{T}}\mathrm{i}_{dqm}\right]_0^{T_{mech}}}^{supplied\ energy} \tag{12}$$

Where, $\mathcal{E}_{me}$ (0) is energy stored at t=0 while $\mathcal{E}_{me}(T_{mech}) \geq 0$

Hence above inequality concludes the passivity of the electrical subsystem. As PMSG is considered to be decomposed of two subsystem that are passive. It is clear from the transfer function that mechanical subsystem $\left(\frac{Y_{mech}}{V_{mech}} = \frac{1}{J + X_{vi}}\right)$ is also passive confirming passivity of PMSG as it is composed of interconnected electrical and mechanical passive subsystems with input and output vectors given in Table 1. Parameters details for the PMSG and the wind turbine are provided in Table 2.

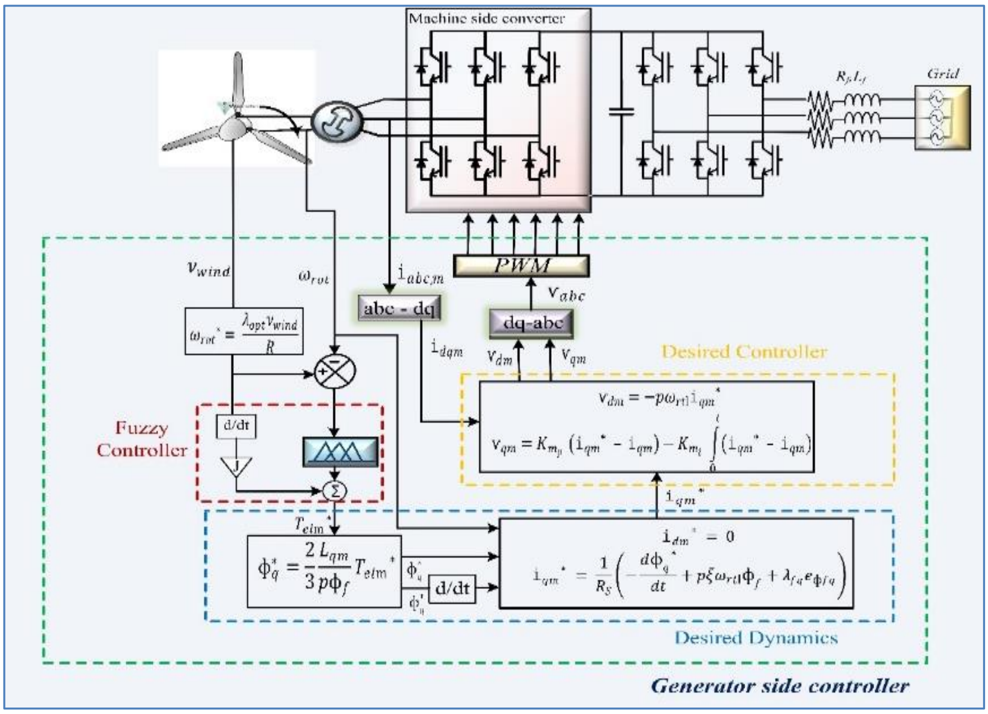

Figure 2. Schematic diagram of proposed fuzzy logic-based passivity generator side controller

Table 1. Electrical and mechanical subsystem input output vectors

Subsystem	Input vector	Output vector
Electrical	$V_{em} = \begin{bmatrix}\mathrm{i}_{dqm}\\ -\omega_{rtl}\end{bmatrix}$	$Y_{em} = \begin{bmatrix}V_{dq}\\ T_{elm}\end{bmatrix}$
Mechanical	$V_{mech} = (-T_{elm} + T_{mech})$	$Y_{mech} = -\omega_{rtl} = \frac{(-T_{elm} + T_{mech})}{J + X_{vi}}$

The proposed flux-oriented current controller based on passivity aims to design desired voltage controller by determining both the reference current $\left(\mathrm{i}_{dqm}{}^{*}\right)$ and the torque $T_{elm}{}^{*}$. Defining the desired vector for flux and its corresponding errors as [20]:

$$\phi_{dq}^* = [\phi_d^* \ \phi_q^*]^T \text{ and } [e_{\phi fd} \ e_{\phi fq}]^T = \phi_{dq} - \phi_{dq}^* \text{ or, } \phi_{dq} = e_{\phi f} + \phi_{dq}^*$$

Substituting ϕ_{dq} in (5) we obtain dynamic equation of error function as in (13).

$$\frac{de_{\phi f}}{dt} + p\omega_{rtl}\, e_{\phi f}\chi = -R_{dq}\mathrm{i}_{dqm}{}^* - \left(\phi_{dq}^* + p\omega_{rtl}\xi\phi_{dq}^*\right) \tag{13}$$

The objective is to determine the $\mathrm{i}_{dqm}{}^*$control input that leads to the error vector $e_{\phi f}$ converging to zero. To analyze system's stability, a function $D(e_{\phi f})$ is introduced that defines reference energy such that (14).

$$D(e_{\phi f}) = \frac{1}{2} e_{\phi f}^T * e_{\phi f} \tag{14}$$

The derivative of $\frac{dD(e_{\phi f})}{dt}$ along (1) leads to (15).

$$\frac{dD(e_{\phi f})}{dt} = -e_{\phi f}{}^T \left(R_{dq}\left(\mathrm{i}_{dqm}{}^*\right) + \frac{d\phi_{dq}^*}{dx}\, p\omega_{rtl}\xi\phi_{dq}^*\right) \left(as\ p\omega_{rtl}\xi e_{\phi f}{}^T e_{\phi f} = 0\right) \tag{15}$$

This leads to controller dynamic for reducing error vector as (16).

$$\mathrm{i}_{dm}{}^* = 0\,;\ \mathrm{i}_{qm}{}^* = \frac{1}{R_S}\left(-\frac{d\phi_q{}^*}{dt} + p\xi\omega_{rtl}\phi_f + \lambda_{fq}e_{\phi fq}\right) \text{ where } \lambda_{fq} > 0 \tag{16}$$

Addition of damping factor λ_{fq}.

By setting the direct current i_{dm} to zero, the PMSG can achieve maximum torque. The flux vector ϕ_{dq} is required to configure the current controller $\mathrm{i}_{dqm}{}^*$. As clear from (16) first term of $\mathrm{i}_{qm}{}^*$ defines the reference dynamics while the second term is added as a damping factor which in turn makes convergence faster along with improving system stability. It also ensures the strict passivity of the closed-loop system. The proposed passivity-based current controller leads to an exponential decay.

Table 2. PMSG & WT parameters for simulations

Rated power	P=1.5MW
Pole pair numbers	p = 40
Stator resistance	Rs=3.18 mΩ
Stator inductance	Ls= 3.07 mH
Moment of inertia	J=10100 kg.m^2
Flux linkage	ϕ =7.0175 wb
WT radius	R = 34.5 m
Inertia (WT)	J = 35100 Kg.m^2
Air density	1.025 kg/m^2
Cp $_{opt}$	0.48

2.2. Reference torque using fuzzy logic controller

The relation between current vector and i_{dqm} and flux ϕ_{dqm} is given as (17).

$$\phi_{dqm} = \begin{bmatrix}\phi_{dm}\\ \phi_{qm}\end{bmatrix} = \left(L_{dqm}\mathrm{i}_{dqm} + \phi_f\right) \tag{17}$$

In order to determine the appropriate control signal $\mathrm{i}_{dqm}{}^*$ it is necessary to compute the flux ϕ_{dq}^* [21]. $\mathrm{i}_{dm} = 0$ as in (17) results in (18).

$$\phi_{qm}^* = L_{qm}\mathrm{i}_{dqm} \tag{18}$$

This equation allows us to calculate the flux reference ϕ_q^* as in (19) by combining (18) and (3).

$$\phi_q^* = \frac{2}{3}\frac{L_{qm}}{p\phi_f} T_{elm}{}^* \tag{19}$$

In the (19), $T_{elm}{}^*$ represents the reference torque. By analysing the mechanical dynamic (18) and setting the rotor speed ω_{rtl} to its desired value, we can compute the desired torque $T_{elm}{}^*$ using (20).

$$T_{elm}{}^* = J_m \frac{d\omega_{rtl}{}^*}{dt} - \chi_{vi}(\omega_{rtl}{}^* - \omega_{rtl}) \tag{20}$$

To address convergence limitations and counter the influence of mechanical parameters (J_m and χ_{vi}) on the open-loop torque formulation, a fuzzy logic controller is utilised [22]. The use of FLC approach aims to reduce static errors, ensure stability, and enhance robustness against parameter variations in the closed-loop system. It accelerates the convergence of the speed tracking error ($\varepsilon_m = \omega_{rtl}{}^* - \omega_{rtl}$) [23]. The fuzzy controller's design involves fuzzification, rule base formulation, and defuzzification, utilizing input signals like speed error ε_m, as show in Figure 3 and its derivative, as in Figure 4 with trapezoidal and triangular membership functions, as in Figure 5. These linguistic variables generate a control structure shown in Figure 6, employing fuzzy sets from Table 3 that are defined as negative big (NB), negative medium (NM), negative small (NS), zero (Z), positive small (PS), positive medium (PM), and positive big (PB).

Table 3. Fuzzy rule table for fuzzy logic controller

E/CE	NB	NM	NS	Z	PS	PM	PB
NB	NB	NB	NB	NB	NM	NS	Z
NM	NB	NB	NB	NM	NS	Z	PS
NS	NB	NB	NM	NS	Z	PS	PM
Z	NB	NM	NS	Z	PS	PM	PB
PS	NM	NS	Z	PS	PM	PB	PB
PM	NS	Z	PS	PM	PB	PB	PB
PB	Z	PS	PM	PB	PB	PB	PB

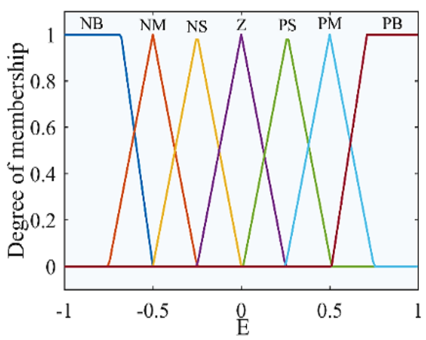

Figure 3. Membership function for input speed error

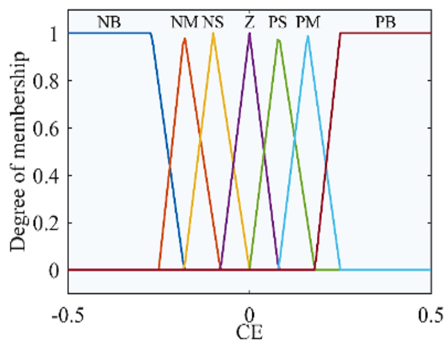

Figure 4. Membership function for input rate of change in speed error

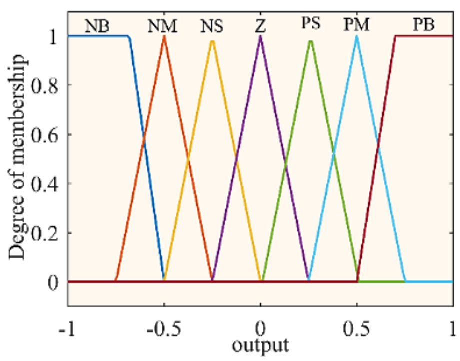

Figure 5. Membership function for output

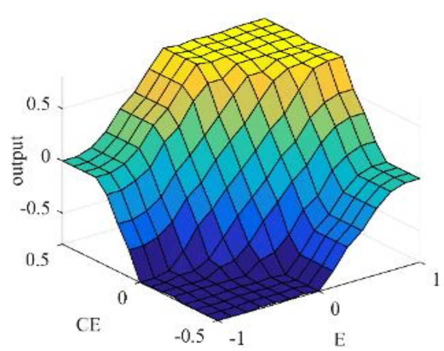

Figure 6. Control surface for FLC

2.3. Grid side controller

The grid-side converter (GSC) as shown in Figure 7 is designed to regulate the DC voltage and inject only active power into the grid while maintaining zero reactive power. This involves controlling inverter d-q frame voltage components (e_d and e_q), grid voltages (v_{gd} and v_{gq}) and d-q frame grid currents (i_{df} and i_{qf}) [24]. Equation for DC link capacitor (V_{dc}) and grid voltage is given by (21) and (22) respectively.

$$C\frac{dV_{dc}}{dt} = \frac{3}{2}\left(\frac{v_{dg}}{V_{dc}} i_{df} + \frac{v_{qd}}{V_{dc}} i_{qf}\right) - i_{dc} \quad (21)$$

$$v_{gd} = e_d - R_{gf}i_{df} + \omega L_{gf}i_{qf} - L_{gf}\frac{di_{fd}}{dt} \; ; \; v_{gq} = e_q - R_{gf}i_{qf} - \omega L_{gf}i_{df} - L_{gf}\frac{di_{fq}}{dt} \quad (22)$$

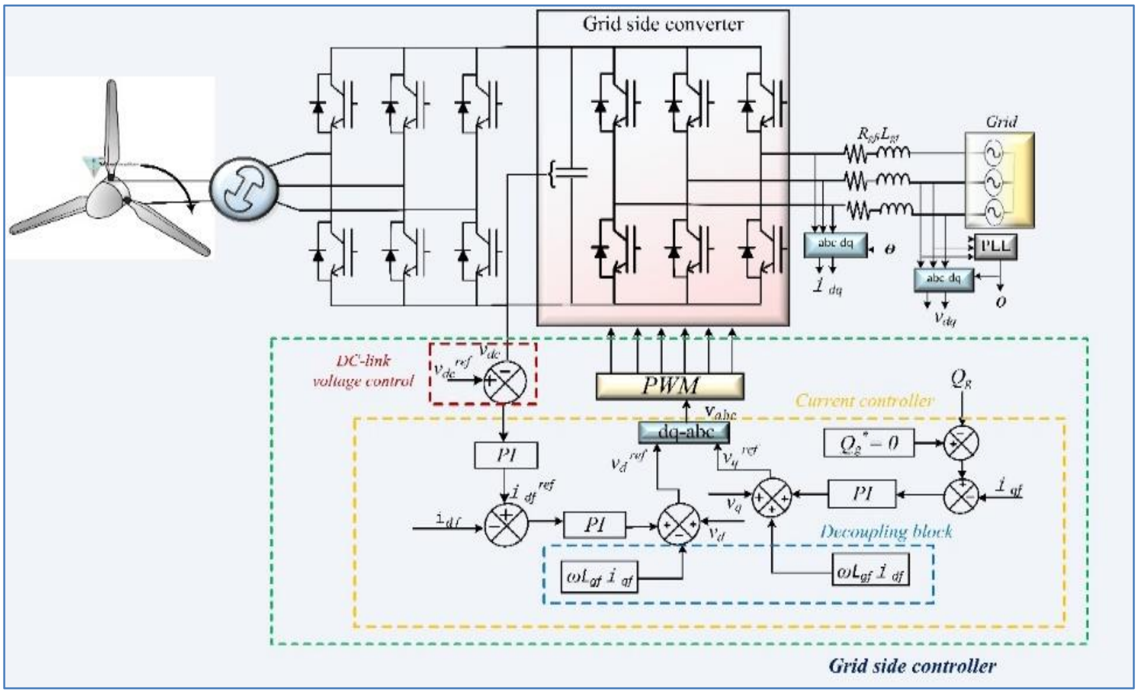

Figure 7. Schematic diagram of grid side controller

This approach generates a desired d-axis current (i_{df}) to ensure a proportional active power exchange between grid and generator based on (i_{df}) while q-axis current (i_{qf}) is determined by generator's reactive power (Q_g). In order to allow only active power injection into the grid, the reference current (i_{qf}^{ref}) is maintained at zero [25] while i_{df}^{ref} , v_{gd}^{ref} and v_{gq}^{ref} are subsequently derived as in (23)-(24).

$$i_{df}^{ref} = K_{dc_p}\left(v_{dc_{ref}} - v_{dc}\right) - K_{dc_i}\int_0^t\left(v_{dc_{ref}} - v_{dc}\right) \quad (23)$$

$$v_{gd}^{ref} = K_{gp}^{d}\left(i_{df}^{ref} - i_{df}\right) - K_{gi}^{d}\int_0^t\left(i_{df}^{ref} - i_{df}\right); v_{gq}^{ref} = K_{gp}^{q}\left(i_{qf}^{ref} - i_{qf}\right) - K_{gi}^{q}\int_0^t\left(i_{qf}^{ref} - i_{qf}\right) \quad (24)$$

The mathematical model of GSC incorporates filter inductance (L_{gf}), filter resistance (R_{gf}), network angular frequency (ω), and DC-link capacitor (C). The (25) for active power ($\mathcal{P}_g$) and reactive power (Q_g) depends on grid voltages and currents. The GSC's functioning focuses on ensuring stability and efficient power delivery into the grid.

$$\mathcal{P}_g = \frac{3}{2} v_{gq}i_{df} \; ; \; Q_g = \frac{3}{2} v_{gd}i_{qf} \quad (25)$$

Figure 8 presents the MATLAB based simulation diagram for the overall system. It unifies the generator side and grid-side controller to illustrate the comprehensive control strategy implemented in the proposed PMSG-based WECS. The figure clearly indicates the input, output variables and switching scheme as per the generator side and grid side control scheme discussed.

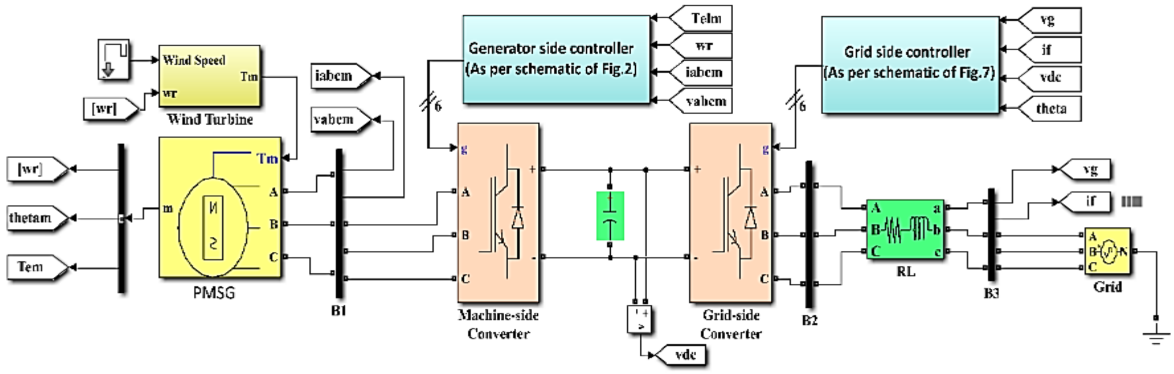

Figure 8. Simulation setup integrating generator and grid side controller for proposed PMSG based WECS

3. RESULTS AND DISCUSSION

In the comprehensive simulations, a 1.5 MW direct-drive PMSG-based wind energy conversion system (WECS) is considered. The evaluation encompasses two scenarios: one assesses system performance under varying wind conditions, while the other examines performance under both changing wind conditions and parametric variations. Additionally, the FLPBC controller is compared with the conventional PI controller.

3.1. Case I: Performance analysis for variable wind and fixed parameters

Figure 9 illustrates a change in wind speed, shifting from 7 m/s at t = 1 sec to 12 m/s at t = 8 sec. In this analysis, it is considered that the system can receive power without limitations, indicating an unrestricted capacity for power absorption. This suggests that the system can fully utilize the generated power. The generator establishes the reference speed, and the DC-bus maintains a consistent reference voltage of 1150 V, with zero kVAR reactive power reference. Table 4 provides the detailed information about various parameter values and constants used.

3.1.1. Fixed parameter analysis

In Figure 10, a stable voltage at the DC-bus is seen that remains consistent despite changes in wind conditions. The system's response, as depicted in Figure 11, reveals those variations in speed lead to consecutive fluctuations in torque at the generator terminal. With increasing wind speed, there's a rise in mechanical power input to the PMSG, resulting in a power imbalance. Consequently, the wind turbine accelerates, as illustrated in Figure 12. Notably, Figure 13 clearly demonstrates the FLPBNC controller's effectiveness in maintaining an optimal Cp value (0.48) when compared to the PI controller. Assessing FLPBNC's performance under stochastic wind conditions, as presented in Figure 14, highlights its capacity to notably minimize the deviation of the power coefficient from its optimum value, as displayed in Figure 15, in contrast to the PI controller. Figure 16 presents a comparative analysis of reactive power (Q_g) fluctuations between the PI controller and the proposed FLPBNC. Notably, FLPBNC exhibits a peak error of 0.6×10^{-4} , which is lower than the PI controller's 1.3×10^{-4}, indicating its superior convergence speed.

3.2. Case 2: Performance analysis for variable wind and variable parameters

3.2.1. Robustness analysis

The controller's effectiveness is evaluated under conditions of simultaneous variation in stator resistance (Rs) and generator inertia (J), with a 100% change in set parameter values. Various simulation outcomes are presented to illustrate the transient responses concerning electromagnetic torque, reactive power regulation, and DC-voltage regulation. Three distinct scenarios for parameter adjustments are investigated: i) 1.5Rs, J; ii) Rs, 1.5J; and iii) 2Rs, 2J; as a means to thoroughly assess the robustness of the FLPBNC.

It is evident from Figures 17, 18, and 19 that even a 100% change in Rs and J does not affect the convergence of DC bus voltage, reactive power regulation as well as generated torque. Similarly, in Figures 20-22 simulation results for (1.5 Rs, J) are shown for developed electromagnetic torque, reactive power response, and convergence of DC bus voltage while for case (Rs,1.5 J) illustrated in Figures 23 and 24 proves the robustness of controller. Across all three cases, it becomes evident that the proposed controller exhibits minimal sensitivity to parameter variations. This resilience can be attributed to the inclusion of an additional damping gain in the calculation of the reference q-axis current, effectively counterbalancing the impact of these fluctuations.

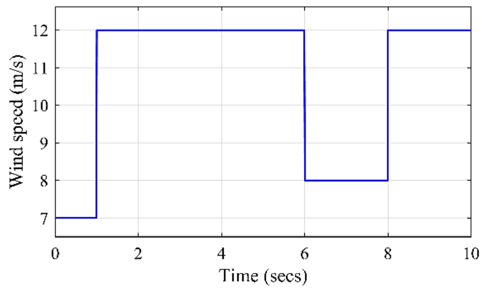

Figure 9. Step change in wind speed

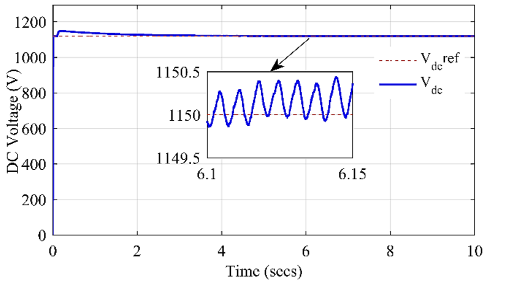

Figure 10. DC voltage response for step wind change

Table 4. Grid side parameters

Parameters	Rating	Parameters	Rating
DC link voltage	V_{dc} = 1150 V	Grid frequency	f = 50 Hz
Capacitor of the DC - link	C = 0.024 F	Grid resistance	R_g = 0.24 pu
Grid voltage	V_g = 575 V	Grid inductance	L_g = 0.24 pu

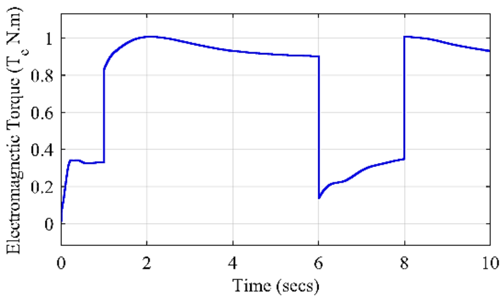

Figure 11. Generated torque for step change in wind

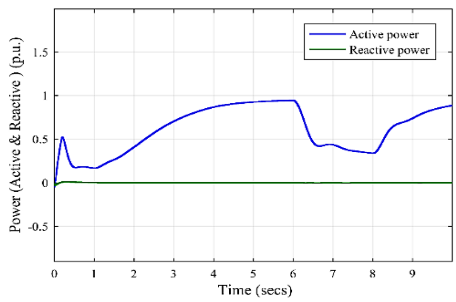

Figure 12. Generated active and reactive power

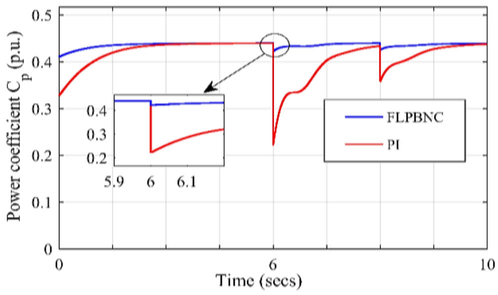

Figure 13. Dynamic change in C_p during step change in wind

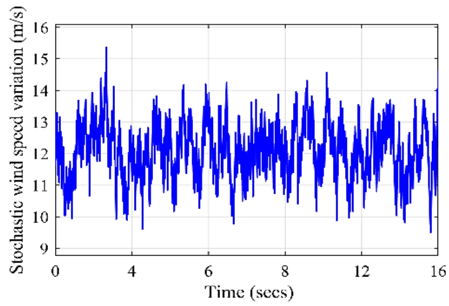

Figure 14. Stochastic change in wind

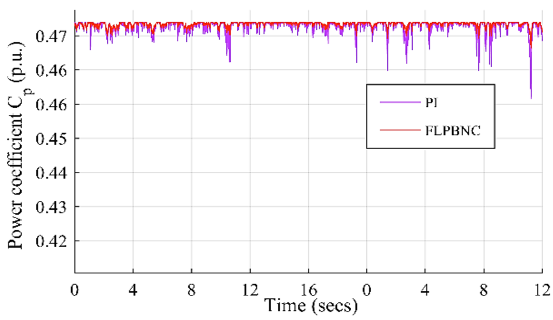

Figure 15. Dynamic change in C_p during stochastic change in wind

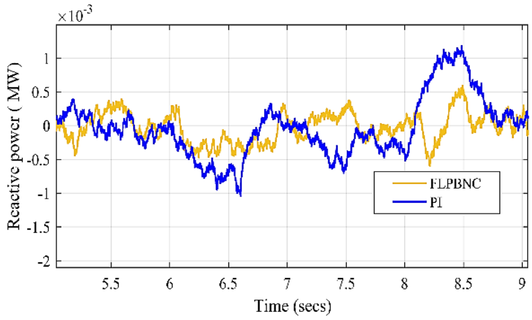

Figure 16. Comparative response of reactive power (PI&FLPBNC)

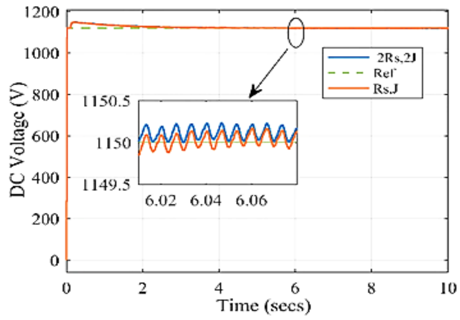

Figure 17. DC voltage response under parameter change (2Rs,2J)

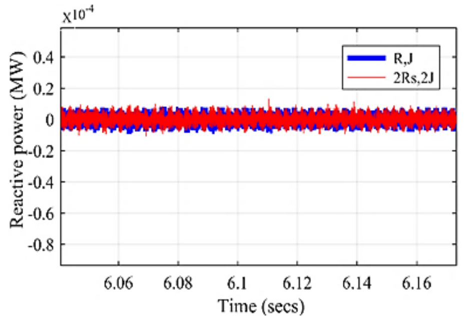

Figure 18. Reactive power under the change in parameter (2Rs,2J)

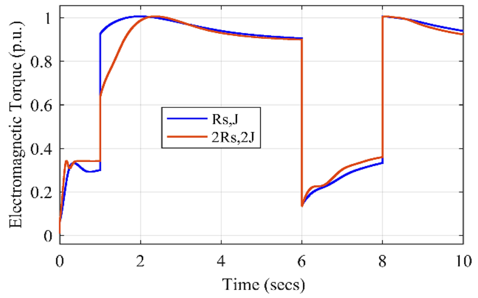

Figure 19. Electromagnetic torque under the change in the parameter (2Rs,2J)

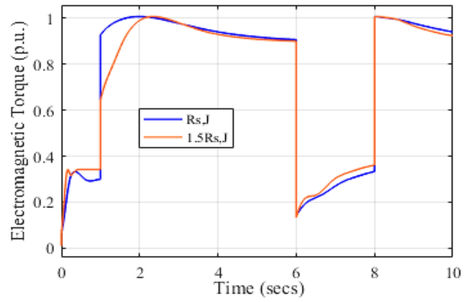

Figure 20. Electromagnetic torque under the change in parameter (1.5Rs, J)

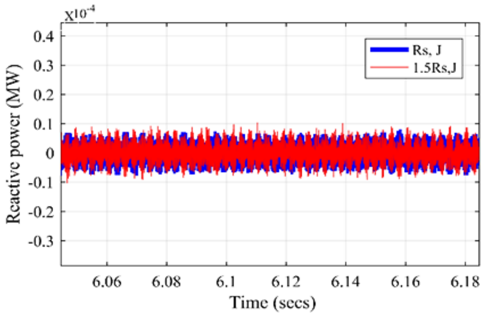

Figure 21. Reactive power for parameter (1.5Rs, J)

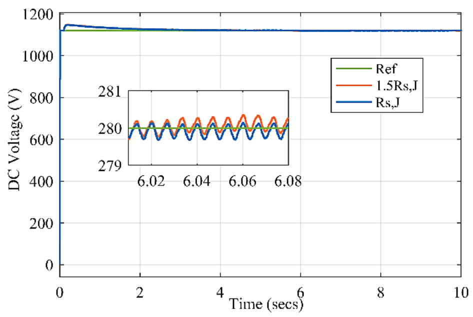

Figure 22. DC bus voltage response under parameter change (1.5Rs, J)

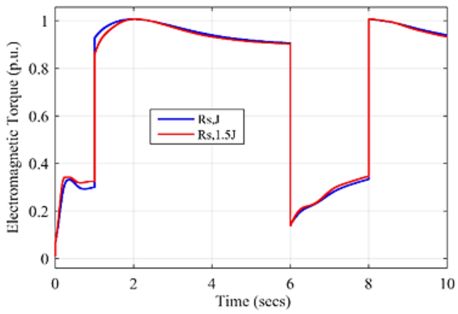

Figure 23. Electromagnetic torque under the change in parameter (Rs,1.5J)

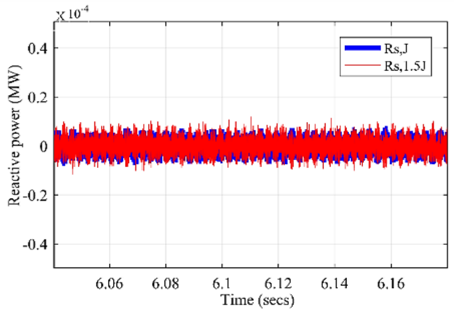

Figure 24. Reactive power under the change in parameter (Rs,1.5 J)

4. CONCLUSION

A hybrid approach combining a passivity-based control with a fuzzy logic controller for a variable-speed wind turbine employing a permanent magnet synchronous generator (PMSG) is proposed. The approach yields precise control over torque, current, and speed parameters within a robust closed-loop system. This integrated controller takes into account the complete PMSG dynamics to enhance wind energy extraction efficiency. Specifically, the fuzzy logic controller is responsible for maintaining consistent rated-speed operations and calculating higher reference torque values. Comprehensive simulation results validate the efficacy of the proposed system, highlighting its swift response in capturing maximum wind power while curbing reactive power generation. A comparative evaluation is performed between the conventional proportional-integral (PI) controller and the proposed fuzzy logic and passivity-based nonlinear controller and (FLPBNC). The outcomes confirm the superiority of the FLPBNC in managing power coefficient variations, particularly during step changes and stochastic fluctuations in wind speed. Moreover, dynamic simulations prove FLPBNC's robustness, revealing minimal deviations in critical parameters like torque, reactive power, and DC link voltage even when subjected to substantial parametric perturbations ranging from 1.5 Rs and 1.5 J up to 2Rs and 2J. These results collectively emphasize the efficiency and stability of the proposed controller in wind energy extraction.

REFERENCES

[1] P. Balakrishnan, M. S. Shabbir, A. F. Siddiqi, and X. Wang, "Current status and future prospects of renewable energy: A case study," *Energy Sources, Part A: Recovery, Utilization and Environmental Effects*, vol. 42, no. 21, pp. 2698–2703, 2020, doi: 10.1080/15567036.2019.1618983.

[2] M. K. K. Prince, M. T. Arif, A. Gargoom, A. M. T. Oo, and M. E. Haque, "Modeling, Parameter Measurement, and Control of PMSG-based Grid-connected Wind Energy Conversion System," *Journal of Modern Power Systems and Clean Energy*, vol. 9, no. 5, pp. 1054–1065, 2021, doi: 10.35833/MPCE.2020.000601.

[3] J. Wang, D. Bo, X. Ma, Y. Zhang, Z. Li, and Q. Miao, "Adaptive back-stepping control for a permanent magnet synchronous generator wind energy conversion system," *International Journal of Hydrogen Energy*, vol. 44, no. 5, pp. 3240–3249, 2019, doi: 10.1016/j.ijhydene.2018.12.023.

[4] A. A. Salem, N. A. N. Aldin, A. M. Azmy, and W. S. E. Abdellatif, "A fuzzy logic-based MPPT technique for PMSG wind generation system," *International Journal of Renewable Energy Research*, vol. 9, no. 4, pp. 1751–1760, 2019, doi: 10.20508/ijrer.v9i4.10138.g7778.

[5] X. Liu, Z. Xu, and J. Zhao, "Combined Primary Frequency Control Strategy of Permanent Magnet Synchronous Generator-Based Wind Turbine," *Electric Power Components and Systems*, vol. 46, no. 14–15, pp. 1704–1718, 2018, doi: 10.1080/15325008.2018.1509916.

[6] F. M. Zaihidee, S. Mekhilef, and M. Mubin, "Robust speed control of pmsm using sliding mode control (smc)-a review," *Energies*, vol. 12, no. 9, 2019, doi: 10.3390/en12091669.

[7] K. Chandrasekaran, M. Mohanty, M. Golla, A. Venkadesan, and S. P. Simon, "Dynamic MPPT Controller Using Cascade Neural Network for a Wind Power Conversion System with Energy Management," *IETE Journal of Research*, vol. 68, no. 5, pp. 3316–3330, 2022, doi: 10.1080/03772063.2020.1756934.

[8] H. Ding, X. Zou, and J. Li, "Sensorless Control Strategy of Permanent Magnet Synchronous Motor Based on Fuzzy Sliding Mode Observer," *IEEE Access*, vol. 10, pp. 36743–36752, 2022, doi: 10.1109/ACCESS.2022.3164519.

[9] Y. Barradi, K. Zazi, M. Zazi, and N. Khaldi, "Control of pmsg based variable speed wind energy conversion system connected to the grid with PI and ADRC approach," *International Journal of Power Electronics and Drive Systems*, vol. 11, no. 2, pp. 953–968, 2020, doi: 10.11591/ijpeds.v11.i2.pp953-968.

[10] A. Ardjal, R. Mansouri, and M. Bettayeb, "Fractional sliding mode control of wind turbine for maximum power point tracking," *Transactions of the Institute of Measurement and Control*, vol. 41, no. 2, pp. 447–457, 2019, doi: 10.1177/0142331218764569.

[11] J. Duan, S. Fan, F. Wu, L. Sun, and G. Wang, "Instantaneous power control of a high speed permanent magnet synchronous generator based on a sliding mode observer and a phase locked loop," *International Journal of Electronics*, vol. 105, no. 6, pp. 923–940, Oct. 2018, doi: 10.1109/IECON.2017.8216337.

[12] M. Makhad, M. Zazi, and A. Loulijat, "Nonlinear control of WECS based on PMSG for optimal power extraction," *International Journal of Electrical and Computer Engineering*, vol. 10, no. 3, pp. 2815–2823, 2020, doi: 10.11591/ijece.v10i3.pp2815-2823.

[13] A. Dali, S. Abdelmalek, A. Bakdi, and M. Bettayeb, "A new robust control scheme: Application for MPP tracking of a PMSG-based variable-speed wind turbine," *Renewable Energy*, vol. 172, pp. 1021–1034, 2021, doi: 10.1016/j.renene.2021.03.083.

[14] P. Mani and Y. H. Joo, "Fuzzy logic-based integral sliding mode control of multi-area power systems integrated with wind farms," *Information Sciences*, vol. 545, pp. 153–169, 2021, doi: 10.1016/j.ins.2020.07.076.

[15] Y. Liao, X. Wang, and F. Blaabjerg, "Passivity-based analysis and design of linear voltage controllers for voltage-source converters," *IEEE Open Journal of the Industrial Electronics Society*, vol. 1, no. 1, pp. 114–126, 2020, doi: 10.1109/OJIES.2020.3001406.

[16] Z. Hamodat, I. K. Hussein, and B. A. Nasir, "An Accurate Efficiency Calculation for PMSG Utilized in Renewable Energy Systems," *Journal of Robotics and Control (JRC)*, vol. 4, no. 4, pp. 458–465, 2023, doi: 10.18196/jrc.v4i4.18441.

[17] A. Benmouna, M. Becherif, D. Depernet, and M. A. Ebrahim, "Novel Energy Management Technique for Hybrid Electric Vehicle via Interconnection and Damping Assignment Passivity Based Control," *Renewable Energy*, vol. 119, pp. 116–128, 2018, doi: 10.1016/j.renene.2017.11.051.

[18] M. Hassan, C.-L. Su, F.-Z. Chen, and K.-Y. Lo, "Adaptive passivity-based control of a DC–DC boost power converter supplying constant power and constant voltage loads," *IEEE Transactions on Industrial Electronics*, vol. 69, no. 6, pp. 6204–6214, Jun. 2022, doi: 10.1109/TIE.2021.3086723.

[19] B. Yang *et al.*, "Passivity-based sliding-mode control design for optimal power extraction of a PMSG based variable speed wind turbine," *Renewable Energy*, vol. 119, pp. 577–589, 2018, doi: 10.1016/j.renene.2017.12.047.

[20] H. Zakeri and P. J. Antsaklis, "Recent advances in analysis and design of cyber-physical systems using passivity indices," *27th Mediterranean Conference on Control and Automation, MED 2019 - Proceedings*, pp. 31–36, 2019, doi: 10.1109/MED.2019.8798500.
[21] W. Gil-Gonzalez, A. Garces, and O. B. Fosso, "Passivity-Based Control for Small Hydro-Power Generation with PMSG and VSC," *IEEE Access*, vol. 8, pp. 153001–153010, 2020, doi: 10.1109/ACCESS.2020.3018027.
[22] B. Belkacem, N. Bouhamri, L. A. Koridak, and A. Allali, "Fuzzy optimization strategy of the maximum power point tracking for a variable wind speed system," *International Journal of Electrical and Computer Engineering*, vol. 12, no. 4, pp. 4264–4275, 2022, doi: 10.11591/ijece.v12i4.pp4264-4275.
[23] A. A. Salem, N. A. N. Aldin, A. M. Azmy, and W. S. E. Abdellatif, "Implementation and Validation of an Adaptive Fuzzy Logic Controller for MPPT of PMSG-Based Wind Turbines," *IEEE Access*, vol. 9, pp. 165690–165707, 2021, doi: 10.1109/ACCESS.2021.3134947.
[24] M. S. Eslahi, S. Vaez-Zadeh, and A. Jabbarnejad, "A Comparative Study of Control Methods for Grid Side Converters in PMSG-Based Wind Energy Conversion Systems," *IEEE International Symposium on Industrial Electronics*, vol. 2020-June, pp. 979–984, 2020, doi: 10.1109/ISIE45063.2020.9152427.
[25] P. Chaturvedi and D. K. Palwalia, "PMSG based Standalone Wind Energy Conversion System with Power Quality Enhancement," *International Journal of Renewable Energy Research*, vol. 13, no. 2, pp. 911–919, 2023, doi: 10.20508/ijrer.v13i2.13958.g8764.

BIOGRAPHIES OF AUTHORS

Pallavi Chaturvedi is a research scholar in Department of Electrical Engineering at the Rajasthan Technical University, Kota, Rajasthan, India. She received her B.Tech. in 2002, M.Tech. in 2014 in Electrical Engineering from Rajasthan Technical University, Kota, Rajasthan, India. Her research interests include the field of renewable energy, power electronics, micrograms. She can be contacted at email: pallavichat9@gmail.com.

Dheeraj Kumar Palwalia is a professor in Department of Electrical Engineering at the Rajasthan Technical University, Kota, India. He received the B.Tech. and M.Tech. both from Malviya National Institute of Technology, Jaipur, India in 1996 and 1998, resp.; and Ph.D. degree from Indian Institute of Technology Roorkee, India in 2009. His research interests include the field of power electronics, renewable energy, induction motor drives, micro grid. He can be contacted at email: dkpalwalia@rtu.ac.in.